Synthesis, Characterization, and Reactions of Carbon Dioxide Bridged Iron–Rhenium Complexes

Dorothy H. Gibson,* Ming Ye, John F. Richardson, and Mark S. Mashuta

Department of Chemistry, University of Louisville, Louisville, Kentucky 40292

Received July 8, 1994®

A new μ_2-η^2-CO_2-bridged complex, $CpFe(CO)(PPh_3)(CO_2)Re(CO)_4[P(OEt)_3]$ (**3**), has been characterized. Thermolysis of **3** in benzene at 60 °C occurs with loss of CO from the rhenium center and provides a μ_2-η^3-CO_2-bridged complex, **4a**. Compound **4a** has been characterized by X-ray crystallography (space group $P2_1/n$, $a = 10.229(6)$ Å, $b = 13.737(9)$ Å, $c = 25.25(2)$ Å, $\beta = 99.20(7)°$, $Z = 4$, $\varrho_{calc} = 1.69$ g cm^{-3}, and $R = 0.038$). The structure shows that the rhenium atom has facial geometry and that the phosphorus ligands on iron and rhenium are anti; additionally, the plane of the CO_2 ligand bisects the angle defined by the phosphorus, iron, and carbonyl carbon atoms. Exhaustive thermolysis of **3**, in solution or in the solid state, leads to a different μ_2-η^3-CO_2-bridged complex, **5b**, in which the PPh_3 and $P(OEt)_3$ ligands have exchanged metal centers; **5b** retains facial geometry at rhenium. Attempted thermolysis of **4a** in the solid state under similar conditions resulted in no reaction. Studies of the thermolysis reactions of **3**, in solution, under milder conditions revealed the presence of intermediate compounds, **4b** and **5a**, which isomerized to **5b** as the final product. Compounds **4b** and **5a** also have facial geometry at rhenium. Partial thermolysis of **4a** in solution, in the presence of CO, led to mixtures containing **4b**, **5a**, and **5b**. Reaction of **4a** with $P(OEt)_3$ led to a new μ_2-η^2-CO_2-bridged complex, **6**; reaction of **4a** with CO at room temperature afforded partial conversion to **3**. Thermolysis pathways are proposed in which O–Re bond breaking in the μ_2-η^3 complexes is followed by ligand capture (CO or $P(OEt)_3$), facial to facial rearrangement, or phosphorus ligand exchange between the two metal centers. The thermolysis reactions clearly demonstrate the robust nature of the CO_2 bridging ligands in this series of compounds.

Introduction

Efforts to use carbon dioxide as a building block in organic synthesis depend upon finding catalytic methods for its fixation. Since effective catalytic methods will likely involve transition metals, the organometallic chemistry of CO_2 is receiving much attention.[1] One area of active investigation is the study of carbon dioxide bridged bimetallic complexes in which the metal centers generally have widely differing electron-donor and electron-acceptor properties to facilitate binding of the CO_2 ligand; also, it is believed that CO_2 activation may be achieved through such compounds.[2] Previous investigations have included studies of bimetallic compounds in which a transition metal binds the carboxyl carbon and one or both oxygens are bound to an alkali metal, a main-group metal or another transition metal.[3] In a continuation of our efforts to define the properties of these compounds, we report the synthesis of new iron–rhenium μ_2-η^2-CO_2-bridged complexes, the unique course of their thermolysis reactions, and the characterization of μ_2-η^3-CO_2-bridged complexes derived from these reactions.

Results

As in our previous report with a closely related series,[3t] the first μ_2-η^2 complex in the present study is derived from reaction of $CpFe(CO)(PPh_3)CO_2^-K^+$ (**1**; Cp = η^5-C_5H_5) with a rhenium complex bearing a weakly coordinated BF_4 ligand. Synthesis of *cis*-$Re(CO)_4[P(OEt)_3](F–BF_3)$ (**2**) was accomplished by treating the corresponding methyl complex with $HBF_4{\cdot}Et_2O$ as has been done previously for related compounds;[3t,4] both **2** and **3** have been characterized by elemental analysis and by spectral data which support the assignment of the cis geometry. In particular, ^{13}C NMR data for both compounds show three small J_{PC} values and one large J_{PC} value (approximately 80 Hz) for the resonances of the terminal carbonyls on the rhenium center; the large coupling is characteristic of carbonyls trans to a phosphorus ligand.[5] Synthesis of the bridged bimetallic complex is shown in eq 1. As with the earlier compounds of this type prepared by us[3t] or with the related homobimetallic complexes of the μ_2-η^2 type,[3l,q] the infrared DRIFTS spectrum (diffuse reflectance infrared fourier transform spectroscopy; see Experimental Section) of **3** shows a lowered carboxylate carbonyl stretch-

® Abstract published in *Advance ACS Abstracts,* September 15, 1994.

(1) (a) *Catalytic Activation of Carbon Dioxide*; Ayers, W. M., Ed.; ACS Symposium Series 363; American Chemical Society: Washington, DC, 1988. (b) Behr, A. In *Aspects of Homogeneous Catalysis*; Ugo, R., Ed.; D. Reidel: Dordrecht, The Netherlands, 1988; Vol. 6, p 59. (c) Braunstein, P.; Matt, D.; Nobel, D. *Chem. Rev.* **1988**, *88*, 747. (d) Behr, A. *Angew. Chem., Int. Ed. Engl.* **1988**, *27*, 661. (e) *Carbon Dioxide Activation by Metal Complexes*; Behr, A.; VCH: Weinheim, Federal Republic of Germany, 1988. (f) Walther, D. *Coord. Chem. Rev.* **1987**, *79*, 135.

(2) (a) Fachinetti, G.; Floriani, C.; Zanazzi, P. F. *J. Am. Chem. Soc.* **1978**, *100*, 7405. (b) Gambarotta, S.; Arena, F.; Floriani, C.; Zanazzi, P. F. *J. Am. Chem. Soc.* **1982**, *104*, 5082.

0276-7333/94/2313-4559$04.50/0

$$CpFe(CO)(PPh_3)CO_2^-K^+ + Re(CO)_4[P(OEt)_3](F{-}BF_3) \longrightarrow$$

1 2

$$CpFe(CO)(PPh_3)\text{–}C(=O)\text{–}O\text{–}Re(CO)_4[P(OEt)_3] \quad (1)$$

3

ing band at 1497 cm^{-1} (see Figure 1, spectrum a). The ^{13}C NMR spectrum of **3** shows the iron-bound carbonyl carbons as doublets at δ 221.01 and 211.61; on the basis of comparisons with related compounds,[3t] the higher field doublet is assigned to the carboxyl carbon. The rhenium-bound carbonyl carbons appear as doublets at δ 188.82 (J_{PC} = 13.7 Hz), 188.60 (J_{PC} = 13.6 Hz), 187.40 (J_{PC} = 8.7 Hz), and 186.31 (J_{PC} = 92.0 Hz), consistent with a cis geometry at the rhenium center.[5] The ^{31}P spectrum shows singlets at δ 113.80 and 80.40 for the phosphorus ligands bound to rhenium and iron, respectively.

Thermolysis of **3** in benzene at 60 °C converts it cleanly to the corresponding μ_2-η^3 complex, $CpFe(CO)(PPh_3)(CO_2)Re(CO)_3[P(OEt)_3]$ (**4a**), which has been characterized by elemental analysis, spectral data, and X-ray crystallography (see Figure 2, Tables 1–3, and discussion below). The structural data for **4a** show significant shortening of the iron–carboxyl carbon bond in comparison to the closely related μ_2-η^2 complex characterized previously.[3t] Enhanced carbene character in the iron–carboxyl carbon bond is suggested by the ^{13}C NMR spectrum of the compound, which shows a downfield shift of this carbon to δ 245.94 while the terminal carbonyl on iron shifts, only slightly, to δ 219.70. The remaining terminal carbonyls, on rhenium, are doublets

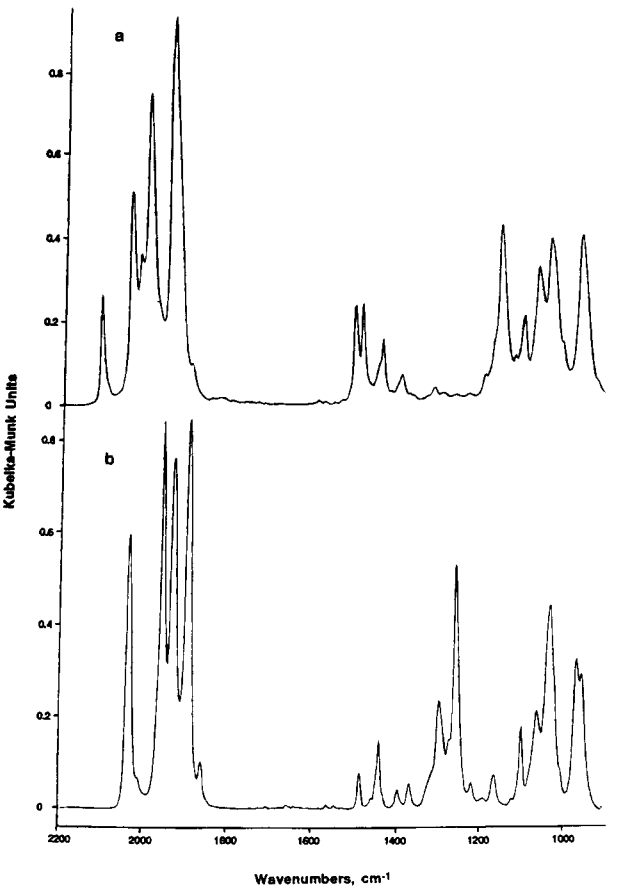

Figure 1. DRIFTS spectra of compound **3** (a) and compound **4a** (b) obtained as dispersions in KCl.

of equal intensities at δ 196.32, 196.21, and 192.91, the last having a very large coupling constant. This pattern is consistent with a facial arrangement[5] of the carbonyl ligands at the rhenium center, which was confirmed by X-ray crystallography. Since the carboxyl oxygens occupy adjacent coordination sites on rhenium and the phosphite ligand is cis to these, there are two possible isomers having facial geometry at the rhenium atom. However, spectral data show evidence of only one isomer, and the structural data indicate that it is the one in which the phosphorus ligands on the two metal centers are anti to one another. DRIFTS data for **4a**, obtained as a KCl dispersion, show ν_{OCO} bands at 1435 and 1252 cm^{-1} (see Figure 1, spectrum b); the band positions are quite similar to those reported for the previous series of μ_2-η^3 iron–rhenium complexes.[3t] The ^{31}P spectrum of **4a** shows singlets at δ 133.50 and 75.60 for the phosphorus ligands on rhenium and iron, respectively.

Since we had observed previously[3t] that μ_2-η^2 to μ_2-η^3 conversions could also occur in solid-state thermolyses, a sample of **3** was sealed in a glass tube, under vacuum, and heated to 80 °C for 6 h. The reaction product, obtained in 63% yield after purification, showed IR bands at 1437 and 1259 cm^{-1} in DRIFTS spectra and low-field doublets at δ 244.69 and 217.40 in ^{13}C NMR spectra, again indicating formation of a μ_2-η^3 complex but one distinct from compound **4a** obtained in the solution thermolysis. The remaining carbonyl ligands in the ^{13}C NMR spectrum showed a pattern which was again consistent with facial geometry at the rhenium atom (see Experimental Section). Also, the ^{31}P spec-

(3) (a) Grice, N.; Kao, S. C.; Pettit, R. *J. Am. Chem. Soc.* **1979**, *101*, 1627. (b) Maher, J. M.; Lee, G. R.; Cooper, N. J. *J. Am. Chem. Soc.* **1982**, *104*, 6797. (c) Audett, J. D.; Collins, T. J.; Santarsiero, B. D.; Spies, G. H. *J. Am. Chem. Soc.* **1982**, *104*, 7352. (d) Forschner, T.; Menard, K.; Cutler, A. *J. Chem. Soc., Chem. Commun.* **1984**, 121. (e) Lee, G. R.; Cooper, N. J. *Organometallics* **1985**, *4*, 794. (f) Barrientos-Penna, C. F.; Gilchrist, A. B.; Klahn-Oliva, H.; Hanlan, A. J. L.; Sutton, D. *Organometallics* **1985**, *4*, 478. (g) Tso, C. T.; Cutler, A. R. *J. Am. Chem. Soc.* **1986**, *108*, 6069. (h) Giuseppetti, M. E.; Cutler, A. R. *Organometallics* **1987**, *6*, 970. (i) Gibson, D. H.; Ong, T.-S. *J. Am. Chem. Soc.* **1987**, *109*, 7191. (j) Lee, G. R.; Maher, J. M.; Cooper, N. J. *J. Am. Chem. Soc.* **1987**, *109*, 2956. (k) Senn, D. R.; Gladysz, J. A.; Emerson, K.; Larsen, R. D. *Inorg. Chem.* **1987**, *26*, 2737. (l) Bennett, M. A.; Robertson, G. B.; Rokicki, A.; Wickramasinghe, W. A. *J. Am. Chem. Soc.* **1988**, *110*, 7098. (m) Pilato, R. S.; Geoffroy, G. L.; Rheingold, A. L. *J. Chem. Soc., Chem. Commun.* **1989**, 1287. (n) Pilato, R. S.; Housmekerides, C. E.; Jernakoff, P.; Rubin, D.; Geoffroy, G. L.; Rheingold, A. L. *J. Am. Chem. Soc.* **1990**, *9*, 2333. (o) Field, J. S.; Haines, R. J.; Sundermeyer, J.; Woolam, S. F. *J. Chem. Soc., Chem. Commun.* **1990**, 985. (p) Gibson, D. H.; Richardson, J. F.; Ong, T.-S. *Acta Crystallogr.* **1991**, *C47*, 259. (q) Torreson, I.; Michelin, R. A.; Marsella, A.; Zanardo, A.; Pinna, F.; Strukul, G. *Organometallics* **1991**, *10*, 623. (r) Vites, J. C.; Steffey, B. D.; Giuseppetti-Dery, M. E.; Cutler, A. R. *Organometallics* **1991**, *10*, 2827. (s) Gibson, D. H.; Ong, T.-S.; Ye, M. *Organometallics* **1991**, *10*, 1811. (t) Gibson, D. H.; Ye, M.; Richardson, J. F. *J. Am. Chem. Soc.* **1992**, *114*, 9716. (u) Szalda, D. J.; Chou, M. H.; Fujita, E.; Creutz, C. *Inorg. Chem.* **1992**, *31*, 4712. (v) Field, J. S.; Haines, R. J.; Sundermeyer, J.; Woolam, S. F. *J. Chem. Soc., Dalton Trans.* **1993**, 2735. (w) Gibson, D. H.; Richardson, J. F.; Mbadike, O. P. *Acta Crystallogr.* **1993**, *B49*, 784. (x) Pinkes, J. R.; Cutler, A. R. *Inorg. Chem.* **1994**, *33*, 759. (y) Gibson, D. H.; Mehta, J. M.; Ye, M.; Richardson, J. F.; Mashuta, M. S. *Organometallics* **1994**, *13*, 1070. (z) Yang, Y.-L.; Chen, J.-D.; Liu, Y.-C.; Cheng, M.-C.; Wang, Y. *J. Organomet. Chem.* **1994**, *467*, C8.

(4) (a) See: Beck, W. *Inorg. Synth.* **1990**, *28*, 1 and references cited therein. (b) Schweiger, M.; Beck, W. *Z. Anorg. Allg. Chem.* **1991**, *595*, 203.

(5) Vaughn, G. D.; Strouse, C. E.; Gladysz, J. A. *J. Am. Chem. Soc.* **1986**, *108*, 1462.

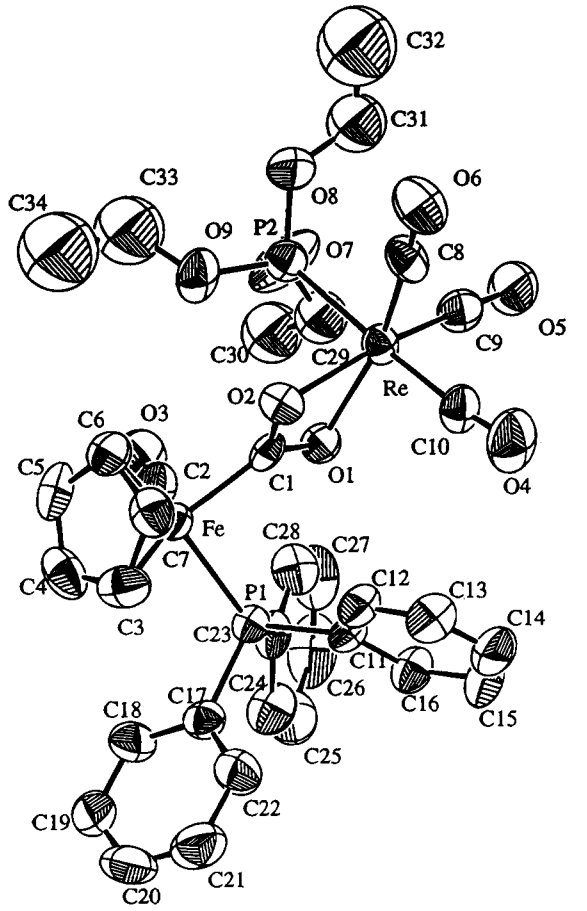

Figure 2. ORTEP drawing of **4a** with thermal ellipsoids shown at the 50% probability level.

Table 1. Summary of Crystallographic Data for $CpFe(CO)(PPh_3)(CO_2)Re(CO)_3[P(OEt)_3]$ (4a)

formula	$FeReP_2O_9C_{34}H_{35}$
fw	891.65
cryst syst	monoclinic
space group	$P2_1/n$
a, Å	10.229(6)
b, Å	13.737(9)
c, Å	25.25(2)
β, deg	99.20(7)
V, Å^3	3501(5)
Z	4
ϱ_{calc}, g/cm^3	1.69
cryst dimens, mm	0.10 × 0.15 × 0.25
cryst descripn	yellow block
μ(Mo Kα), cm^{-1}	40.12
abs corr (method)	DIFABS
transmissn factors: min/max	0.952/1.041
radiation	Mo Kα (λ = 0.710 93 Å)
diffractometer	CAD4
monochromator	graphite cryst
temp, °C	22
scan type	$\omega-2\theta$
scan range	0.80 + 0.35 tan θ
scan speed, deg/min	1–5
max 2θ, deg	50
no. of unique rflns collected	6473
no. of rflns included ($I_o > 3\sigma(I_o)$)	4273
no. of params	424
computer hardware	Silicon Graphics Iris Indigo
computer software	teXsan
extinctn coeff	extinctn could not be refined
agreement factors[b]	
R	0.038
R_w	0.039
function minimized	$\sum w(\|F_o\| - \|F_c\|)^2$
GOF	1.90
weighting scheme	$[\sigma^2(F_o)]^{-1}$
high peak in final diff map, e	1.25

[a] $R = \sum||F_o| - |F_c||/\sum|F_o|$; $R_w = (|F_o| - |F_c|)^2/\sum wF_o^2]^{1/2}$.

trum showed singlets at δ 179.60 and 23.30, indicating profound changes in the phosphorus ligand environments. Elemental analysis of the new compound, which will be identified as **5b**, was consistent with the same molecular formula as that of **4a**. Since both μ_2-η^2-CO_2- and μ_2-η^3-CO_2-bridged complexes are subject to cleavage by strong electrophiles, a sample of **5b** was treated with $HBF_4{\cdot}Et_2O$. The ether-insoluble product from this reaction had properties which were identical with those of an authentic sample of $CpFe(CO)_2[P(OEt)_3]^+BF_4^-$, providing clear evidence that the iron and rhenium centers had *exchanged phosphorus ligands* during the solid-state thermolysis of **3**. Thus, **5b** should be formulated as the μ_2-η^3 complex $CpFe(CO)[P(OEt)_3](CO_2)Re(CO)_3(PPh_3)$. Ligand exchange between metal centers in CO_2-bridged complexes has not been observed previously.

Additional thermolysis reactions have been conducted in order to try to understand how different products could result from solution and solid-state reactions. Incomplete thermolysis of **3** in the solid state (1 h at 70 °C) afforded a mixture containing unreacted **3** together with **4a**, **5b**, and two additional compounds. One of these, designated as **4b**, showed two ^{31}P resonances which were closely similar to those of **4a**, while the other one (designated as **5a**) showed two resonances which were quite close to those of **5b** (see Experimental Section and Figure 3). Examination of the ^{13}C NMR spectral properties of the mixture in comparison to those of compounds **3**, **4a**, and **5b** allowed us to identify the carbonyl resonances due to the new compounds and to determine that the geometry at the rhenium center remained facial in these thermolysis products also (two doublets with small J_{PC} values and one with a very large J_{PC} value for each compound). Since compound **4a** has been shown to have an anti arrangement of the two phosphorus ligands (see Figure 2), the only available facial geometry at the rhenium atom for **4b** would place the phosphorus ligands on the two metal centers in closer proximity (syn). Also, the most stable arrangement for the final product, **5b**, should be one in which the phosphorus ligands are again anti; this leads to the conclusion that **5a** must have a syn geometry with respect to the phosphorus ligands on adjacent metal centers (see Discussion). A series of thermolysis experiments was then conducted at 80 °C with **3** in solution in toluene followed by ^{31}P NMR; these results are profiled in Figure 3. Spectrum a, taken after 5 min, clearly shows the conversion of a large amount of **3** into **4a** (**3** to **4a** ratio approximately 2:1). After 10 min (spectrum b), **3** had decreased and resonances for **4b** and **5a** were present in addition to those of **4a** (relative percentages of **3**, **4a**, **4b**, and **5a**: 26%, 67%, 4% and 3%, respectively). After 15 min (spectrum c), the resonances for one further compound (**5b**) were evident and the relative percentages of **3**, **4a**, **4b**, **5a**, and **5b** were 20%, 61%, 8%, 9%, and 2%, respectively. After 25 min, (spectrum d), compounds **3**, **4a**, and **4b** were greatly diminished and the relative amounts of **5a** and **5b** had changed so that **5b** was predominant. After 50 min (spectrum e), compound **3** had disappeared and **5b** had become the dominant compound in the mixture; the relative percentages of **4a**, **4b**, **5a**, and **5b** were 5%, 15%, 17%, and 63%, respectively. These experiments indicated that the thermolysis pathways in solution and in

Table 2. Positional and Isotropic Thermal Parameters for Non-H Atoms in 4a

atom	x	y	z	B_{eq},[a] Å^2
Re	0.02455(3)	0.12009(3)	−0.25029(1)	3.444(8)
Fe	−0.16842(10)	0.11544(9)	−0.10134(4)	3.06(3)
P(1)	−0.0818(2)	0.2567(2)	−0.06958(9)	3.12(5)
P(2)	0.0709(2)	−0.0480(2)	−0.22640(10)	3.92(6)
O(1)	0.0374(5)	0.1462(4)	−0.1652(2)	3.5(1)
O(2)	−0.1493(4)	0.1114(4)	−0.2132(2)	3.7(1)
O(3)	0.0468(7)	−0.0102(5)	−0.0559(3)	6.4(2)
O(4)	−0.0212(7)	0.3331(5)	−0.2879(3)	7.8(2)
O(5)	0.3028(6)	0.1440(5)	−0.2762(3)	7.2(2)
O(6)	−0.0668(7)	0.0566(5)	−0.3657(3)	6.9(2)
O(7)	0.2045(7)	−0.0738(5)	−0.1893(3)	8.1(2)
O(8)	0.0749(6)	−0.1223(5)	−0.2741(3)	6.2(2)
O(9)	−0.0387(6)	−0.0979(4)	−0.1995(3)	5.5(2)
C(1)	−0.0899(7)	0.1275(5)	−0.1657(3)	2.9(2)
C(2)	−0.0375(8)	0.0435(6)	−0.0734(4)	4.2(2)
C(3)	−0.3595(8)	0.1597(8)	−0.0934(5)	5.4(3)
C(4)	−0.3191(10)	0.0857(9)	−0.0558(4)	5.7(3)
C(5)	−0.2947(10)	0.0036(7)	−0.0848(5)	5.8(3)
C(6)	−0.3196(9)	0.0255(7)	−0.1394(4)	4.8(3)
C(7)	−0.3608(8)	0.1232(8)	−0.1451(4)	4.9(2)
C(8)	−0.0295(9)	0.0827(7)	−0.3219(3)	4.6(2)
C(9)	0.1946(9)	0.1345(6)	−0.2655(3)	4.4(2)
C(10)	−0.0038(8)	0.2551(7)	−0.2701(4)	4.5(2)
C(11)	−0.0765(7)	0.3546(5)	−0.1174(3)	3.1(2)
C(12)	−0.1717(8)	0.3597(6)	−0.1631(3)	4.2(2)
C(13)	−0.1763(9)	0.4376(7)	−0.1982(4)	4.8(3)
C(14)	−0.082(1)	0.5071(7)	−0.1906(4)	5.9(3)
C(15)	0.0138(10)	0.5036(7)	−0.1464(4)	5.7(3)
C(16)	0.0177(8)	0.4283(6)	−0.1096(4)	4.4(2)
C(17)	−0.1740(8)	0.3133(6)	−0.0214(3)	3.6(2)
C(18)	−0.1805(9)	0.2673(7)	0.0266(4)	4.6(2)
C(19)	−0.252(1)	0.3064(8)	0.0635(4)	6.0(3)
C(20)	−0.317(1)	0.3928(10)	0.0520(5)	7.1(4)
C(21)	−0.313(1)	0.4410(8)	0.0048(5)	6.8(4)
C(22)	−0.2408(9)	0.4009(7)	−0.0321(4)	5.2(3)
C(23)	0.0853(8)	0.2558(6)	−0.0316(3)	3.8(2)
C(24)	0.1197(9)	0.3108(7)	0.0147(4)	5.4(3)
C(25)	0.247(1)	0.3117(9)	0.0419(4)	6.8(4)
C(26)	0.343(1)	0.2584(10)	0.0240(5)	7.2(4)
C(27)	0.3133(10)	0.2028(9)	−0.0212(5)	6.7(3)
C(28)	0.1826(9)	0.2023(7)	−0.0497(3)	4.8(3)
C(29)	0.2917(10)	−0.0092(8)	−0.1584(5)	6.3(3)
C(30)	0.352(1)	−0.0531(9)	−0.1078(5)	8.5(4)
C(31)	0.180(1)	−0.1197(9)	−0.3050(5)	8.2(4)
C(32)	0.155(2)	−0.180(1)	−0.3497(7)	14.6(7)
C(33)	−0.036(1)	−0.1996(8)	−0.1833(6)	11.1(5)
C(34)	−0.136(2)	−0.2281(9)	−0.1611(8)	14.6(7)

[a] $B_{eq} = {}^8/_3\pi^2(U_{11}(aa^*)^2 + U_{22}(bb^*)^2 + U_{33}(cc^*)^2 + 2U_{12}aa^*bb^* \cos\gamma + 2U_{13}aa^*cc^* \cos\beta + 2U_{23}bb^*cc^* \cos\alpha)$.

Table 3. Selected Bond Distances and Bond Angles for Compound 4a

Distances (Å)			
Re—O(1)	2.163(5)	C(9)—O(5)	1.185(9)
Re—O(2)	2.143(5)	C(10)—O(4)	1.164(10)
Re—C(8)	1.878(10)	Fe—P(1)	2.227(3)
Re—C(9)	1.858(9)	Fe—C(1)	1.932(7)
Re—C(10)	1.934(9)	Fe—C(2)	1.730(9)
Re—P(2)	2.416(3)	Fe—C(3)	2.092(9)
C(1)—O(1)	1.322(8)	Fe—C(4)	2.107(9)
C(1)—O(2)	1.274(8)	Fe—C(5)	2.095(9)
C(2)—O(3)	1.163(9)	Fe—C(6)	2.088(8)
C(8)—O(6)	1.167(10)	Fe—C(7)	2.104(9)
Angles (deg)			
P(2)—Re—O(1)	86.0(1)	C(8)—Re—C(9)	88.4(4)
P(2)—Re—O(2)	88.8(2)	C(8)—Re—C(10)	90.2(4)
O(1)—Re—O(2)	59.9(2)	C(9)—Re—C(10)	87.1(4)
O(1)—Re—C(8)	164.8(3)	P(1)—Fe—C(1)	91.8(2)
O(1)—Re—C(9)	106.1(3)	P(1)—Fe—C(2)	96.5(3)
O(1)—Re—C(10)	94.8(3)	C(1)—Fe—C(2)	89.6(4)
O(2)—Re—C(8)	105.5(3)	Fe—C(1)—O(1)	123.2(5)
O(2)—Re—C(9)	166.0(3)	Fe—C(1)—O(2)	125.2(5)
O(2)—Re—C(10)	93.9(3)	Fe—C(2)—O(3)	175.8(8)
Re—O(1)—C(1)	93.1(4)	O(1)—C(1)—O(2)	111.3(6)
Re—O(2)—C(1)	95.6(4)		

the solid state were parallel. Furthermore, it was clear that **5a** was formed before **5b**. Structural rearrangements such as these have not been observed previously in thermolyses of CO_2-bridged compounds.

Additional experiments have been done to try to clarify the thermolysis pathways. Heating **4a** in the solid state at 85 °C for 3 days (conditions more forcing than those used for the complete conversion of **3** to **5b**) caused *no isomerization* of the compound to occur. Thermolysis experiments conducted on **4a** in solution provided additional insight. Heating **4a** in toluene for 80 min at 70 °C followed by examination of the ^{31}P NMR spectrum of the sample showed that approximately 28% of it had been converted to **4b**, **5a**, and **5b**; some sample degradation also occurred. However, in a tandem experiment, in which the solution of **4a** was saturated with CO prior to heating, approximately 64% of it was converted to the three thermolysis products; a small amount of sample degradation again occurred during this thermolysis. When a sample of **4a** was saturated with CO and allowed to stand at room temperature for 2 days, examination of the ^{31}P NMR spectrum showed that approximately one-third of it had converted back to **3**, with smaller amounts of **5a** and **5b** also being produced. Clearly **4a** can be converted to the other thermolysis products only when CO is available (from sample degradation or addition). Efforts to promote the thermal reorganization of **5b**, with and without CO, were unsuccessful. Furthermore, efforts to obtain samples enriched in **4b** or **5a** in order to follow the isomerization profiles of these compounds were unsuccessful. Thus, we cannot determine whether **4b** and **5a** require CO to isomerize to **5b**, although this seems unlikely (see Discussion below).

Treatment of **4a** with 1 equiv of triethyl phosphite, over 20 min at room temperature, was sufficient to convert **4a** into a new compound, **6**. The elemental analysis and spectral properties of **6** are consistent with its formulation as a μ_2-η^2-CO_2-bridged complex, $CpFe(CO)(PPh_3)(CO_2)Re(CO)_3[P(OEt)_3]_2$. DRIFTS data show the carboxylate carbonyl at 1510 cm^{-1}, as expected for a CO_2-bridged compound of this type; solution spectra show the terminal carbonyls as strong bands at 2035, 1964, and 1900 cm^{-1}, consistent with a facial arrangement of these ligands.[6] The ^{13}C NMR spectrum shows the terminal carbonyl on iron as a doublet at δ 222.23 and the carboxyl carbon as a doublet of triplets centered at δ 207.25 while the terminal carbonyls on rhenium appear as pairs of doublets at δ 192.84, 192.19, and 191.83; the first two pairs of doublets exhibit one small and one very large J_{PC} value, consistent with one cis and one trans relationship between each carbonyl carbon and the two phosphorus ligands, while the third one shows two small J_{PC} values, consistent with cis relationships of this carbonyl to the two phosphorus ligands. This pattern, also, is consistent with facial geometry of the CO ligands. Compound **6** is much more thermally stable than **3**, showing no loss of CO under conditions which would have converted **3** to **4a**. Treatment of **4a** with triphenylphosphine, under conditions similar to those used with $P(OEt)_3$, showed significant

(6) Bond, A. M.; Colton, R.; McDonald, M. E. *Inorg. Chem.* **1978**, *17*, 2842.

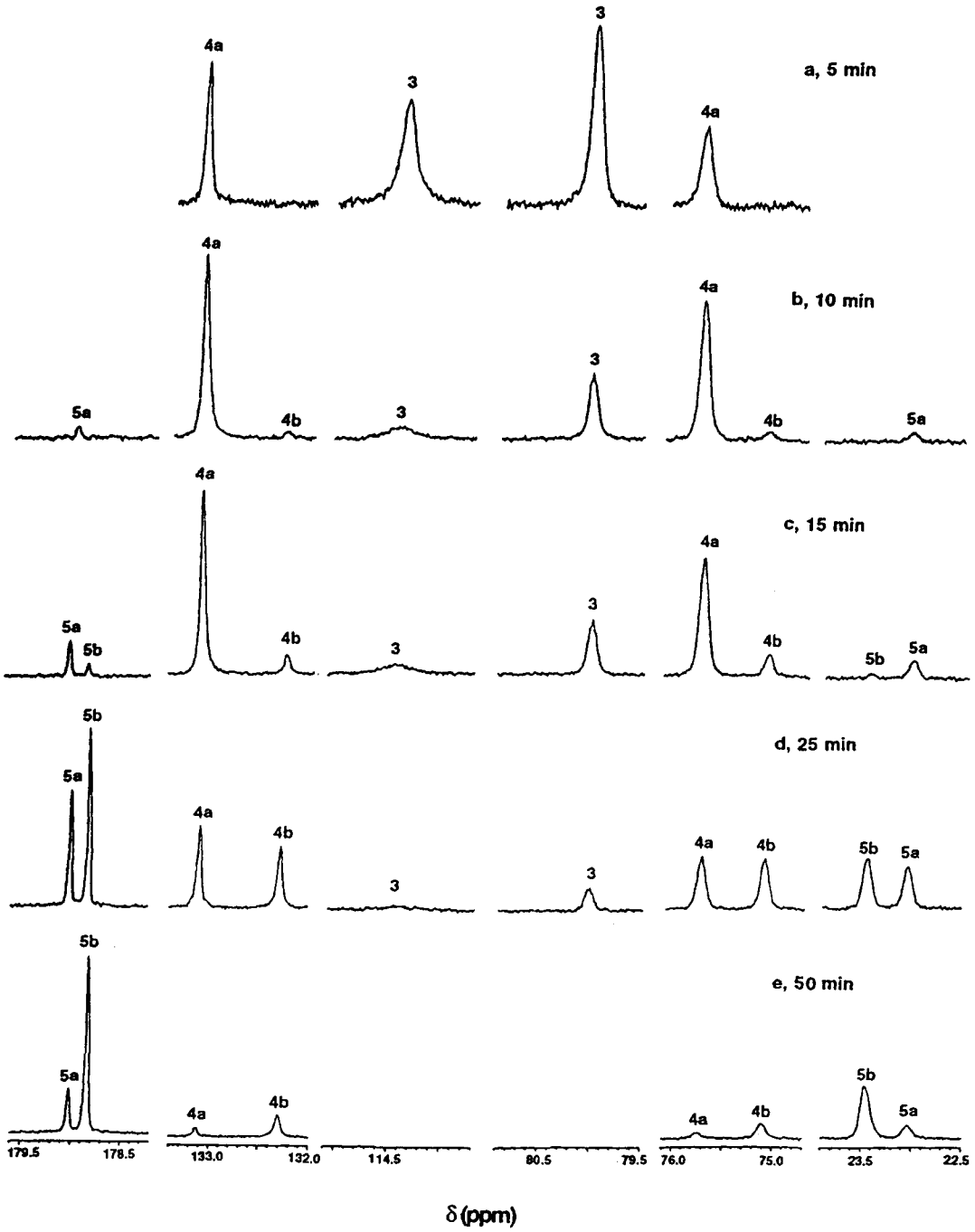

Figure 3. ^{31}P NMR spectra of the thermolysis of **3** at 80 °C in toluene as a function of time.

conversion to a product whose spectral properties were similar to those of **6**; this product has not been characterized.

Discussion

The structure of **4a** is represented in the ORTEP diagram shown in Figure 2. Crystallographic data are summarized in Table 1; Table 2 contains selected bond distances and bond angles. Note that the iron–carboxyl carbon bond length in **4a** is 1.932(7) Å, which is shortened in comparison to that in the closely related μ_2-η^2 complex $CpFe(CO)(PPh_3)(CO_2)Re(CO)_4(PPh_3)$[3t] (1.994(3) Å) and essentially equal to that of the μ_2-η^3 iron–tin complex $CpFe(CO)(PPh_3)(CO_2)SnPh_3$ (**7**)[3p] (1.931(5) Å). The carboxyl C–O bond lengths in **4a** (1.322(8) and 1.274(8) Å) are also closely similar to those in **7** (1.305(6) and 1.270(6) Å). Major differences arise, however, when the carboxyl oxygen to metal bond lengths in these two complexes are compared. The O–Re bond lengths in **4a** are similar at 2.163(5) and 2.143(5) Å, whereas O–Sn bond lengths in **7** are very unequal at 2.123(4) and 2.342(4) Å. Carboxyl O–C–O bond angles also differ in the two compounds: 111.3(6)° in **4a** and 113.4(6)° in **7**. These differences parallel structural differences observed by us in related μ_2-η^3-CO_2-bridged complexes derived from a rhenium metallocarboxylate.[3y] Thus, the carboxyl C–O bond lengths in $Cp^*Re(CO)(NO)(CO_2)Re(CO)_3(PPh_3)$ (**8**; $Cp^* = \eta^5$-C_5Me_5) are nearly equal, as are the O–Re bond lengths, but the corresponding bond lengths in $Cp^*Re(CO)(NO)(CO_2)SnPh_3$ (**9**) are highly unsymmetrical, particularly the carboxyl oxygen to tin bond lengths. Figure 4

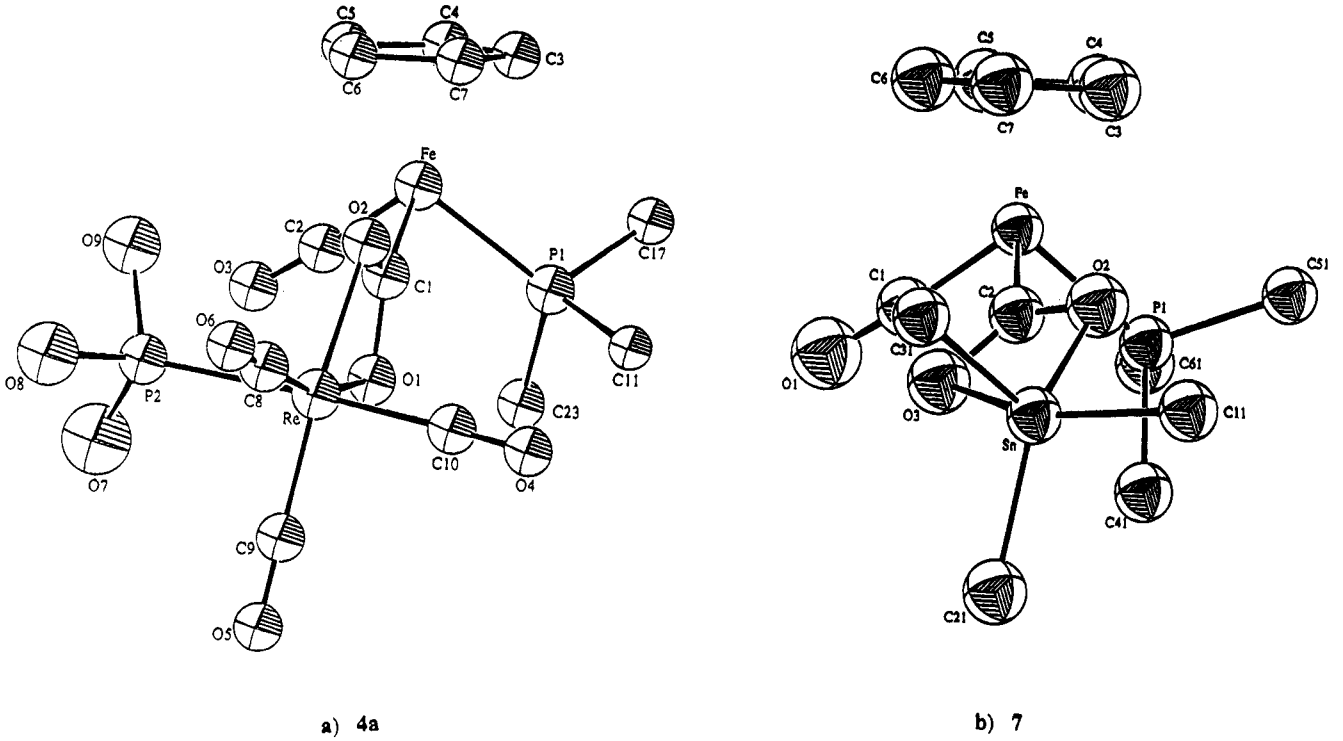

a) 4a b) 7

Figure 4. ORTEP diagrams of **4a** and **7**. Atoms are shown as idealized spheres. The tin and phosphorus atoms are shown with α-bonded atoms only for clarity.

contains ORTEP diagrams of **4a** and **7** which clearly demonstrate the differences in orientation of the bridging CO_2 ligand in the two compounds. In **4a**, the plane defined by the atoms of the carboxyl group bisects the angle defined by the iron atom, P(1), and C(2), while in the iron–tin complex, the plane of the carboxyl group is coplanar with the Fe–C–O plane. While the orientations of the carboxyl ligand in **8** and **9** also differ from one another, the differences do not parallel the orientations in **4a** and **7**.

An indication that **4a** and **7** might have very different solid-state structures came from comparisons of the ^{13}C NMR chemical shifts of the carboxyl carbons in the two compounds: 245.94 ppm in **4a** and 228.16 ppm in **7**. Although this downfield shift might suggest enhanced carbene character in the iron–carboxyl bond for **4a**, metal–carboxyl carbon bond length should be a better indicator of carbene character. The crystallographic data show that this bond in **4a** is essentially equal in length to the one in **7**. However, the internal O–C–O angle in **4a** is smaller than the one in **7**. Similarly, this angle is smaller in **8** than it is in **9**, even though these exhibit very similar rhenium–carboxyl carbon bond lengths.[3y] The related rhenium–tungsten complex $Cp^*Re(CO)(NO)(CO_2)WCp_2^+$, characterized by Geoffroy,[3m,n] shows a slightly shorter Re–C bond but much lower chemical shift for the carboxyl carbon than for **8** (243.1 ppm) and has a much smaller O–C–O angle (106(3)°). On the basis of these comparisons, it seems that the carboxyl carbon chemical shift position is very sensitive to the internal carboxyl O–C–O bond angle, although other factors may also be involved.

Consideration of the thermolysis results described above leads us to suggest the pathway shown in Scheme 1 in order to account for the isomerizations involving the μ_2-η^3 complexes. Conversion of **4a** to **4b** or **5a** to **5b** requires only a facial to facial rearrangement of carbonyl ligands on the rhenium atom. Such rearrangements in octahedral complexes have been observed several times.[7] It is typical to invoke a five-coordinate intermediate in which reorganization of the carbonyl ligands takes place prior to collapse back to the isomeric facial isomer;[8] the presence of this type of intermediate has been unambiguously demonstrated for a manganese carbonyl complex recently.[9] From the results discussed above, it is apparent that an O–Re bond in **4a** is easily broken by substitution of CO or $P(OEt)_3$; bond breaking and CO ligand reorganization could be involved in some of the isomerizations observed here. However, the failure of **4a** to undergo isomerization under thermolysis conditions in the solid state which would have readily converted **3** to **5b** makes it clear that this mechanism cannot account for all of the isomerizations which we have observed. Thus, direct facial to facial rearrangement seems unlikely to occur in this series of compounds except with conversions of syn isomers to their anti counterparts (e.g., **5a** to **5b**). On the basis of our observations with **4a**, anti to syn isomerization requires CO and thus must go backward, through a μ_2-η^2 complex, before providing the less stable, and presumably syn, isomer. It is compound **4b**, not **4a**, that is critical to the phosphorus ligand exchange between the two metal centers which yields **5a**. From the results shown in Figure 3, it is clear that **5a** is formed before **5b**; also, as spectra d and e indicate, syn to anti isomerization of **5a** to **5b** appears to occur readily. Neither $P(OEt)_3$ nor PPh_3 is observed under solution thermolysis conditions; also, the addition of either of

(7) Howell, J. A. S.; Burkinshaw, P. M. *Chem. Rev.* **1983**, *83*, 557.
(8) Lichtenberger, D. L.; Brown, T. L. *J. Am. Chem. Soc.* **1978**, *100*, 366.
(9) (a) Mason, M. R.; Verkade, J. G. *J. Am. Chem. Soc.* **1991**, *113*, 6309. (b) Mason, M. R.; Verkade, J. G. *Organometallics* **1992**, *11*, 1514.

Scheme 1. Proposed Thermolysis Pathways

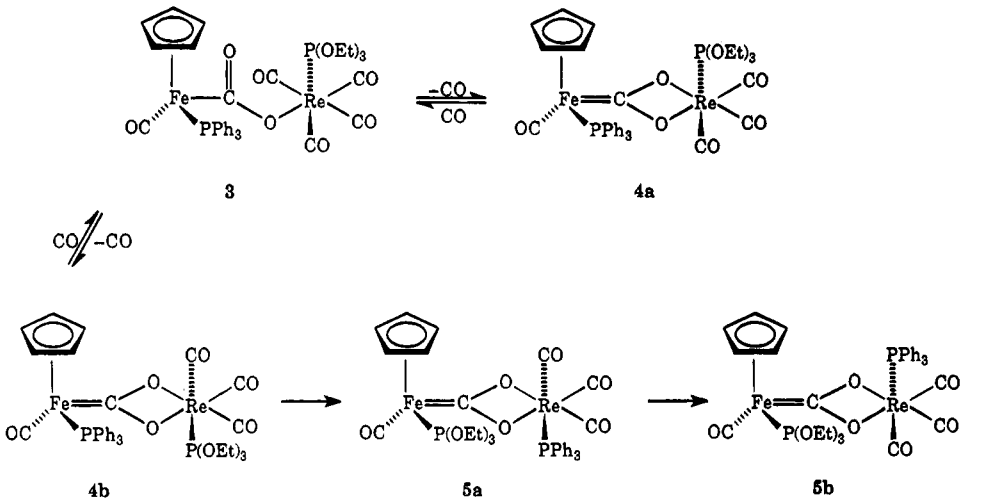

these compounds does not promote the isomerization of **4a** to any of the thermolysis products.

One driving force for the ligand exchange may be the need to place the stronger σ-donor, triphenylphosphine, on the more electron-deficient rhenium atom. However, it is clear that differences in ligand electron donor/acceptor characteristics, alone, do not explain the different behavior of this system as compared to two other systems studied by us previously. Thus, thermolyses of $CpFe(CO)(PPh_3)(CO_2)Re(CO)_4(L)$ with L = CO or $P(OPh)_3$ lead to straightforward loss of CO on rhenium with no structural rearrangements and no ligand exchanges between metal centers.[3t] We believe that the answer lies in the special orientation of the bridging carboxyl group in **4b**, which is expected to parallel that in the crystallographically characterized **4a** except for the placement of the $P(OEt)_3$ ligand in a syn position. Figure 4 shows the geometry of **4a** and **7** from a different perspective, in which differences in carboxyl orientation relative to the cyclopentadienyl ligand are apparent. In **4a**, and presumably **4b**, the orientation of the carboxyl ligand is such that breaking the longer O(1)–Re bond would create a coordination vacancy on rhenium that would be near to the PPh_3 ligand on iron, thus allowing its migration to Re. Rotation about the Fe–carboxyl carbon bond would allow the freed carboxyl oxygen, O(1), to move around and displace $P(OEt)_3$, which can then migrate to the vacant site on iron, thus providing the new μ_2-η^3 complex. The two phosphorus ligands would remain syn in the new complex, thus creating **5a**. Scheme 2 illustrates this proposed reorganization pathway.[10]

Perhaps even more remarkable than the ligand exchange is the fact that the carboxyl bridge remains intact throughout the reorganizations taking place on the two metal centers. The lability of the bridging CO_2 ligand is clearly dependent upon the basicity of the metal center to which the carboxyl carbon is bonded; it is apparent from this and previous work that the $CpFe(CO)(PPh_3)_3$ fragment binds CO_2 irreversibly, unlike $CpFe(CO)_2$.[3b,d,e] The precise role played by the second metal, the one binding one or both of the carboxyl oxygens, in the lability of the bridged complexes is less clear. However, it is apparent from the results described in the present work, as well as in the previous related work,[3t] that increasing the electron density on the second metal center by the substitution of more strongly electron-donating ligands raises the activation energy for the μ_2-η^2 to μ_2-η^3 conversions.

In our previous reports on CO_2-bridged complexes, we have made efforts to correlate structural data with solid-state IR spectral data obtained by the DRIFTS method;[3s,t,y] these efforts are continued in the present work. In contrast to a recent report,[3x] we have not reported any data on ν_{OCO} bands in our compounds from "thin film" spectra. In assigning bands on all compounds with the $CpFe(CO)(PPh_3)$ fragment, as we indicated previously,[3s] it is important to note that all such compounds show two characteristic bands in the middle region of the IR spectrum. One of these bands appears at about 1480 cm^{-1} and the other at approximately 1430 cm^{-1}; Figure 1 shows the DRIFTS spectra of compounds **3** and **4a**. In close similarity with the related compounds reported previously,[3t] the spectrum of μ_2-η^2 complex **3** (spectrum a) shows ν_{OCO} bands at 1497 and 1144 cm^{-1} in addition to the two characteristic bands in the middle region. In **4a** the ν_{OCO} bands have shifted to 1435 and 1252 cm^{-1}; thus, the first band (asymmetric O–C–O stretching) overlaps with the lower of the two characteristic bands, enhancing its intensity, as we have reported for other similar compounds.[3s,t] However, note that the DRIFTS data for **4a** differ from those of the iron–tin complex **7**,[3s] which shows bands at 1432 and 1174 cm^{-1}, again signaling different structural types for the two compounds. Differences of this type were noted with the rhenium metallocarboxylates **8** and **9**.[3y] The DRIFTS spectrum of **5b** is similar to that of **4a**, showing ν_{OCO} bands at 1437 and 1259 $cm.^{-1}$ The ν_{OCO} bands for the μ_2-η^2 complex **6** appear at 1510 and 1140 cm^{-1} as expected because of the close relationship to **3**. The higher frequency bands in this region for **3** and for **6** are also quite similar to the carboxyl carbonyl stretching frequencies reported by Bennett[3l] and by Strukul[3q] for μ_2-η^2-carbon dioxide bridged platinum–platinum complexes. It is interesting to note, however, the significantly different positions of the asymmetric ν_{OCO} bands reported for the first compounds of this type to be described. Thus, Collins[3c] reported bands at approxi-

(10) A reviewer has suggested that the freed O(1) might play a role in displacing the PPh_3 ligand from iron and in helping to control the stereochemical outcome of the rearrangement.

Scheme 2. Proposed Phosphorus Ligand Exchange Pathway

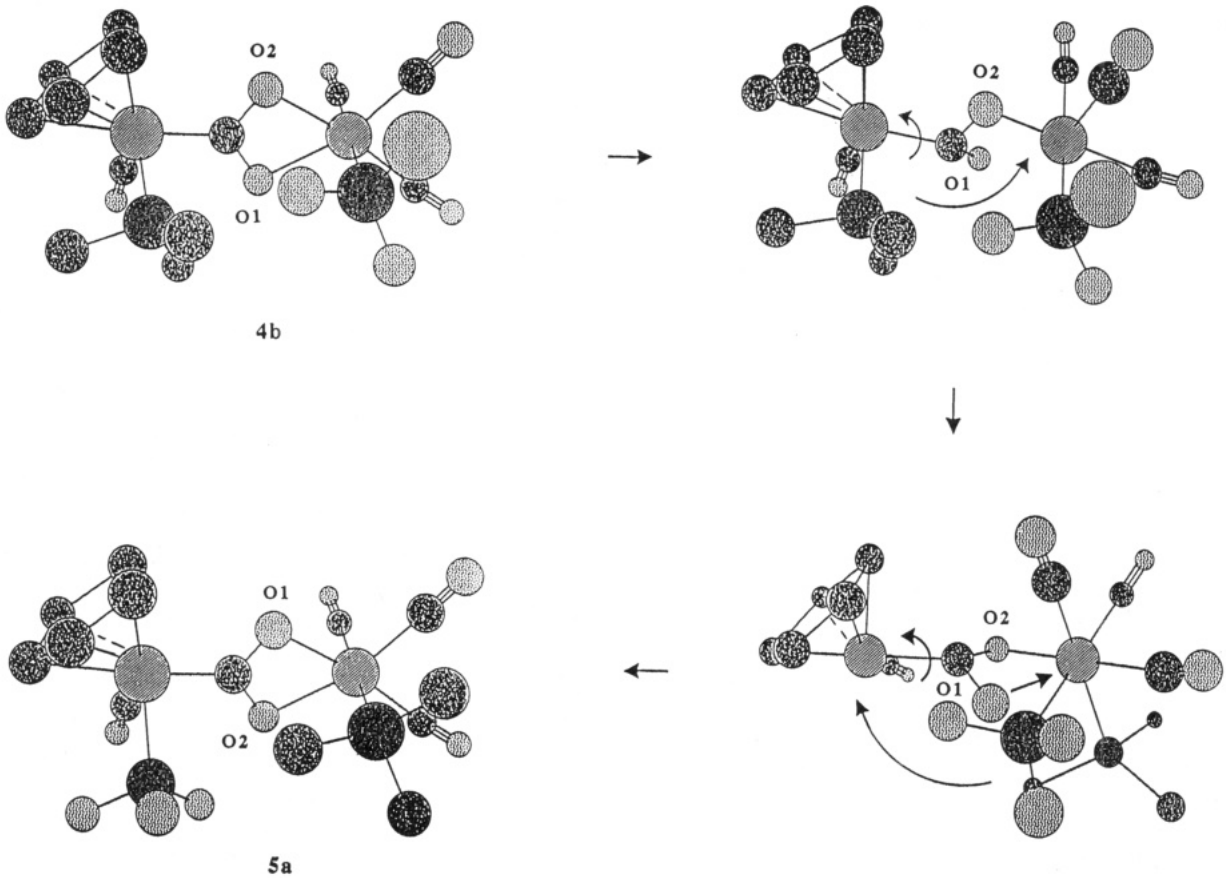

mately 1580 cm^{-1} in two CO_2-bridged iridium–osmium compounds; however, these compounds also had a bridging oxo ligand in each case and should be regarded as five-membered dimetallalactones which would be expected to have higher carboxyl carbonyl stretching frequencies than noncyclic systems (in the same manner that lactones have higher carbonyl stretching frequencies than simple organic esters[11]). Also, the μ_2-η^2-CO_2-bridged ruthenium–ruthenium complex structurally characterized recently by Haines[3v] shows the carbon dioxide ligand bridging two bonded metal centers. The compound, with a four-membered dimetallalactone unit, has an extremely short carboxyl carbonyl C–O bond (1.06(3) Å) and exhibits a band at 1710 cm^{-1} accordingly.

Experimental Section

General Data. Reactions and manipulations were carried out under an atmosphere of prepurified nitrogen in Schlenkware or in a Vacuum Atmospheres glovebox (with Dri-Train). All glassware was dried in the oven before use. Reagent grade solvents dichloromethane, chloroform, carbon tetrachloride, anhydrous diethyl ether, and acetone were used as received. Benzene, toluene, hexane, and pentane were dried over concentrated sulfuric acid and fractionally distilled before use. Solvents used in the glovebox were distilled under nitrogen from the following drying agents: sodium benzophenone ketyl for diethyl ether and tetrahydrofuran (THF); P_2O_5 for dichloromethane, pentane, hexane, benzene, and toluene; calcium hydride for methanol and acetone. Rhenium carbonyl was obtained from Strem Chemical Co. Tetrafluoroboric acid–diethyl ether complex, trifluoromethanesulfonic acid, bromine, methyllithium (1.6 M in ether), triphenylphosphine, triethyl phosphite, silver tetrafluoroborate, benzene-d_6, acetone-d_6, and chloroform-d were obtained from Aldrich. Dichloromethane-d_2 and toluene-d_8 were obtained from Cambridge Isotope Laboratories or Aldrich. Hydrogen bromide was obtained from Matheson Gas Products Inc. and used as received. Anhydrous $(\eta^5\text{-}C_5H_5)Fe(CO)(PPh_3)CO_2^-K^+$ [3s] and $BrRe(CO)_5$[11] were prepared as described previously. Spectral data were obtained on the following instruments: FT-NMR, Bruker AMX-500; IR, Mattson Galaxy series FT-IR 5000 and Perkin-Elmer 599B. Diffuse reflectance[14] IR data were obtained from dispersions of the compounds in KCl with a DRIFTS accessory (Spectra Tech, Inc., Barnes Analytical Division) for the FT-IR. ^1H and ^{13}C NMR chemical shifts were referenced to tetramethylsilane; ^{31}P NMR chemical shifts were referenced to external 85% H_3PO_4. Melting points were obtained on a Thomas-Hoover capillary melting point apparatus and are uncorrected. Elemental analyses were performed by Midwest Microlab, Indianapolis, IN.

Synthesis of $(\eta^5\text{-}C_5H_5)Fe(CO)_2[P(OEt)_3]^+BF_4^-$. $(\eta^5\text{-}C_5H_5)Fe(CO)_2I$ (2.00 g, 6.58 mmol) was dissolved in 100 mL of anhydrous ether. The solution was added to a slurry of $AgBF_4$ (1.40 g, 7.19 mmol) in a small amount of ether under nitrogen. The mixture was then stirred for 2 h. A red precipitate was obtained. The solvent was then evaporated. The red product was dissolved in 80 mL of CH_2Cl_2 and refluxed with $P(OEt)_3$ (1.10 g, 1.14 mL, 6.62 mmol) for 24 h under nitrogen. Solvent was then removed, leaving an oily dark residue. An IR spectrum of this residue showed two strong bands at 2068 and 2024 cm^{-1}. Since efforts to crystallize this product were not successful, the oily residue was chromatographed on 100–200 mesh Florisil with elution by 2:1 CH_2Cl_2/hexane. The eluate

(11) Kemp, W. *Organic Spectroscopy*, 3rd ed.; W. H. Freeman: New York, 1991; Chapter 2.
(12) Reimann, R. H.; Singleton, E. *J. Organomet. Chem.* **1973**, *59*, 309.
(13) teXsan: Single Crystal Structure Analysis Software, Version 1.6 (1993), Molecular Structure Corp., The Woodlands, TX 77381.
(14) Griffiths, P. W.; de Haseth, J. A. *Fourier Transform Infrared Spectroscopy*; Wiley: New York, 1986; Chapter 5.

was concentrated and chilled to −20 °C overnight. Yellow crystals were obtained; the yield was 0.63 g (23% yield), mp 62–64 °C. Anal. Calcd for $C_{13}H_{20}BF_4FeO_5P$: C, 36.32; H, 4.69. Found: C, 36.18; H, 4.79. IR ν_{CO} (CH_2Cl_2): 2068 (s), 2024 (s) cm^{-1}. ^1H NMR (CD_2Cl_2): δ 5.38 (s), 4.15 (quintet, J = 7.2 Hz), 1.38 (t, J = 7.1 Hz). ^{13}C NMR ($CDCl_3$): δ 207.15 (d, J_{PC} = 37.7 Hz), 87.12 (s), 64.47 (d, J_{PC} = 7.4 Hz), 15.78 (d, J_{PC} = 6.7 Hz). ^{31}P NMR (CD_2Cl_2): δ 153.04 (s).

Synthesis of *cis*-BrRe(CO)$_4$[P(OEt)$_3$]. $BrRe(CO)_5$ (2.00 g, 4.92 mmol) was dissolved in 200 mL of $CHCl_3$. $P(OEt)_3$ (0.90 g, 0.93 mL, 5.4 mmol) was added, and the mixture was refluxed under nitrogen for 12–15 h. Solvent was then removed and the crude product was chromatographed on 100–200 mesh Florisil with hexane as the eluent. After removal of solvent, a colorless liquid was obtained in 92% yield (2.46 g). Anal. Calcd for $C_{10}H_{15}BrO_7PRe$: C, 22.07; H, 2.78. Found: 22.47; H, 2.88. IR ν_{CO} (hexane): 2106 (w), 2024 (m), 2004 (s), 1967 (ms) cm^{-1}. ^1H NMR (acetone-d_6): δ 4.22 (quintet, J = 7.1 Hz), 1.35 (t, J = 7.1 Hz). ^{13}C NMR (acetone-d_6): δ 185.00 (d, J_{PC} = 14.7 Hz), 183.97 (d, J_{PC} = 86.6 hz), 182.38 (d, J_{PC} = 12.2 Hz), 63.67 (d, J_{PC} = 6.6 Hz), 16.12 (d, J_{PC} = 6.5 Hz). ^{31}P NMR (acetone-d_6): δ 101.20 (s).

Synthesis of *cis*-CH$_3$Re(CO)$_4$[P(OEt)$_3$]. *cis*-$BrRe(CO)_4[P(OEt)_3]$ (4.50 g, 8.27 mmol) was dissolved in 150 mL of ether and chilled to −20 °C. $LiCH_3$ (excess, 10.3 mL of a 1.6 M ether solution) was added dropwise to the solution under nitrogen over 15 min. Water was then added to destroy excess $LiCH_3$. The ether layer was separated and dried over anhydrous $MgSO_4$. Solvent was then evaporated to dryness to give a liquid product, which was purified by column chromatography on Florisil (100–200 mesh) with hexane as the eluent. The pure product was a colorless liquid, 3.00 g (76% yield). Anal. Calcd for $C_{11}H_{18}O_7PRe$: C, 27.56; H, 3.78. Found: C, 27.62; H, 3.81. IR ν_{CO} (hexane): 2082 (w), 2000 (m), 1981 (s), 1940 (ms) cm^{-1}. ^1H NMR (acetone-d_6): δ 4.07 (quintet, J = 7.1 Hz), 1.32 (t, J = 7.2 Hz), −0.35 (d, J = 9.8 Hz). ^{13}C NMR (acetone-d_6): δ 191.49 (d, J_{PC} = 15.1 Hz), 190.66 (d, J_{PC} = 79.2 Hz), 187.03 (d, J_{PC} = 8.8 Hz), 62.51 (d, J_{PC} = 5.0 Hz), 16.10 (d, J_{PC} = 6.3 Hz), −36.25 (d, J_{PC} = 11.3 Hz). ^{31}P NMR (acetone-d_6): δ 109.80 (s).

Synthesis of *cis*-Re(CO)$_4$[P(OEt)$_3$](F–BF$_3$). In the glovebox, *cis*-$CH_3Re(CO)_4[P(OEt)_3]$ (2.00 g, 4.17 mmol) was dissolved in 20 mL of CH_2Cl_2. $HBF_4{\cdot}Et_2O$ (0.68 g, 0.61 mL, 4.2 mmol) was added dropwise with stirring over 5 min; this addition was accompanied by gas evolution. After another 10 min, solvent was evaporated, leaving an off-white solid which was purified by crystallization in hexane at −60 °C. The white product was collected by filtration; the yield was 2.12 g (92%). Anal. Calcd for $C_{10}H_{15}BF_4O_7PRe$: C, 21.74; H, 2.74. Found: C, 21.81; H, 2.87. IR ν_{CO} (pentane): 2110 (w), 2030 (m), 2008 (s), 1968 (m) cm^{-1}. ^1H NMR (CD_2Cl_2): δ 4.17 (quintet, J = 7.1 Hz), 1.39 (t, J = 7.1 Hz). ^{13}C NMR (CD_2Cl_2): δ 186.91 (d, J_{PC} = 14.6 Hz), 185.67 (d, J_{PC} = 85.7 Hz), 183.76 (q, J_{PC} = 13.2 Hz), 63.80 (d, J_{PC} = 6.3 Hz), 16.13 (d, J_{PC} = 5.0 Hz). ^{31}P NMR (CD_2Cl_2): δ 113.20 (s).

Synthesis of *cis*-(η^5-C$_5$H$_5$)Fe(CO)(PPh$_3$)(CO$_2$)Re(CO)$_4$[P(OEt)$_3$] (3). In the glovebox, *cis*-$Re(CO)_4[P(OEt)_3](F–BF_3)$ (**2**; 1.00 g, 1.81 mmol) was dissolved in 20 mL of CH_2Cl_2 and chilled to −35 °C. $(\eta^5\text{-}C_5H_5)Fe(CO)(PPh_3)CO_2^-K^+$ (0.90 g, 1.82 mmol) was added to the solution in portions over 20 min. The mixture was then filtered, and the filtrate was evaporated to dryness under vacuum. The product was triturated with cold pentane and then dried under vacuum. The yield was 1.23 g (74%). The product was further purified by recrystallization from CH_2Cl_2/pentane at −20 °C to give an analytically pure sample, mp 101–102 °C dec. Anal. Calcd for $C_{35}H_{35}FeO_{10}P_2Re$: C, 45.71; H, 3.84. Found: C, 45.73; H, 3.94. IR ν_{CO} (Nujol): 2092 (w), 2020 (m), 1978 (s), 1930 (m, sh), 1920 (ms) cm^{-1}. IR ν_{CO} (1:4 CH_2Cl_2/hexane): 2086 (w), 2020 (m), 1985 (vs), 1948 (m), 1930 (s) cm^{-1}. IR ν_{OCO} (KCl, DRIFTS): 1497 (w), 1144 (m) cm^{-1}. ^1H NMR (CD_2Cl_2, 0 °C): δ 7.51 (m), 7.36 (m), 4.38 (s), 4.18 (quintet), 1.37 (t). ^{13}C NMR (CD_2Cl_2, −35 °C): δ 221.01 (d, J_{PC} = 31.9 Hz), 211.61 (d, J_{PC} = 32.0 Hz), 188.82 (d, J_{PC} = 13.7 Hz), 188.60 (d, J_{PC} = 13.6 Hz), 187.40 (d, J_{PC} = 8.7 Hz), 186.31 (d, J_{PC} = 92.0 Hz), 137.34 (br), 132.93 (br), 129.90 (s), 127.85 (d, J_{PC} = 8.8 Hz), 84.37 (s), 61.86 (s), 15.93 (s). ^{31}P NMR (CD_2Cl_2, −35 °C): δ 113.80 (s), 80.40 (s).

Thermolysis of 3 in Solution: Synthesis of (η^5-C$_5$H$_5$)Fe(CO)(PPh$_3$)(CO$_2$)Re(CO)$_3$[P(OEt)$_3$] (4a). Compound **3** (0.64 g, 0.70 mmol) was dissolved in 50 mL of C_6H_6 at room temperature under nitrogen. This solution was heated at 60 °C for 1 h under nitrogen. The initial red-orange solution became yellow and slightly cloudy during that time. This mixture was filtered, and the filtrate was evaporated to dryness. The yellow product was transferred into the glovebox, washed with cold pentane at −60 °C, collected by filtration, and dried: 0.55 g (88% yield). The product was recrystallized from CH_2Cl_2/ether at −20 °C; mp 122–125 °C dec. Anal. Calcd for $C_{34}H_{35}FeO_9P_2Re$: C, 45.80; H, 3.96. Found: C, 46.06; H, 4.20. IR ν_{CO} (CH_2Cl_2): 2025 (m), 1930 (vs), 1890 (s) cm^{-1}. IR ν_{OCO} (KCl, DRIFTS): 1435 (w), 1252 (m) cm^{-1}. ^1H NMR (toluene-d_8): δ 7.58 (m), 7.02 (m), 4.41 (s), 4.13 (quintet), 4.11 (quintet), 4.04 (quintet), 4.02 (quintet), 1.16 (t). ^{31}P decoupled ^1H NMR (toluene-d_8) showed methylene proton resonances at δ 4.13 (q, J = 7.4 Hz), 4.11 (q, J = 7.4 Hz), 4.04 (q, J = 6.9 Hz), and 4.02 (q, J = 6.9 Hz). ^{13}C NMR (toluene-d_8): δ 245.94 (d, J_{PC} = 31.0 Hz), 219.70 (d, J_{PC} = 29.5 Hz), 196.32 (d, J_{PC} = 12.3 Hz), 196.21 (d, J_{PC} = 12.0 Hz), 192.91 (d, J_{PC} = 115.9 Hz), 137.31 (d, J_{PC} = 43.9 Hz), 134.03 (d, J_{PC} = 10.1 Hz), 130.48 (d, J_{PC} = 1.9 Hz), 128.74 (d, J_{PC} = 9.8 Hz), 85.71 (s), 61.68 (s), 16.66 (d, J_{PC} = 6.5 Hz). ^{31}P NMR (CD_2Cl_2, −30 °C): δ 133.50 (s), 75.60 (s).

Thermolysis of 3 in the Solid State: Synthesis of (η^5-C$_5$H$_5$)Fe(CO)[P(OEt)$_3$](CO$_2$)Re(CO)$_3$(PPh$_3$) (5b). Compound **3** (0.81 g, 0.88 mmol) was sealed in a glass tube, in vacuo, and heated at 80 °C for 6 h; the color changed from orange to brownish yellow. This crude product was purified by trituration with minimal toluene, filtration, and then addition of cold pentane (−60 °C) in the glovebox to give 0.49 g (63% yield) of a light yellow powder, mp 143–144 °C dec. Anal. Calcd for $C_{34}H_{35}FeO_9P_2Re$: C, 45.80; H, 3.96. Found: C, 45.70; H, 3.83. IR ν_{CO} (CH_2Cl_2): 2020 (s), 1960 (m, br), 1913 (s), 1888 (s) cm^{-1}. IR ν_{OCO} (KCl, DRIFTS): 1437 (w), 1259 (m) cm^{-1}. ^1H NMR (toluene-d_8): δ 7.73 (m), 7.01 (m), 4.13 (quintet), 4.11 (quintet), 4.09 (s), 4.03 (quintet), 4.01 (quintet), 1.14 (t). ^{13}C NMR (toluene-d_8, −20 °C): δ 244.69 (d, J_{PC} = 48.1 Hz), 217.40 (d, J_{PC} = 43.0 Hz), 197.71 (d, J_{PC} = 6.9 Hz), 197.42 (d, J_{PC} = 6.3 Hz), 193.36 (d, J_{PC} = 78.0 Hz), 134.59 (d, J_{PC} = 11.1 Hz), 131.72 (d, J_{PC} = 42.9 Hz), 130.49 (s) (another carbon resonance was obscured by the solvent peak), 83.99 (s), 61.36 (s), 16.04 (d, J_{PC} = 6.0 Hz). ^{31}P NMR (toluene-d_8, −30 °C): δ 179.60 (s), 23.30 (s).

Partial Thermolysis of 3 in the Solid State: Identification of 4b and 5a. Solid **3** (0.15 g, 0.16 mmol) was sealed, in vacuo, and heated at 70 °C for 1 h. An NMR sample was prepared at −30 to −40 °C in CD_2Cl_2. A ^{31}P NMR spectrum was first recorded at −35 °C and showed the presence of four products, **4a**, **4b**, **5a**, and **5b**, with some remaining starting compound **3** in approximately equal amounts. A ^{13}C NMR spectrum was then recorded at the same temperature; in addition to **3**, **4a**, and **5b**, two new compounds, **4b** and **5a**, were present which had spectral properties closely similar to those of **4a** and **5b**, respectively. Compound **4b** had the following resonances of terminal carbonyl and carboxyl groups in its ^{13}C NMR spectrum: δ 245.47 (d, J_{PC} = 31.1 Hz), 219.00 (d, J_{PC} = 28.9 Hz), 195.94 (d, J_{PC} = 12.5 Hz), 195.71 (d, J_{PC} = 11.3 Hz), 193.15 (d, J_{PC} = 115.0 Hz). **5a** showed resonances as follows: δ 244.58 (d, J_{PC} = 48.0 Hz), 216.83 (d, J_{PC} = 43.4 Hz), 197.52 (d, J_{PC} = 10.1 Hz), 196.93 (d, J_{PC} = 8.8 Hz), 190.59 (d, J_{PC} = 69.2 Hz). The ^{31}P NMR showed resonances of **4b** at δ 133.80 (s) and 74.80 (s), and those of **5a** were at δ 180.00 (s) and 21.00 (s). The sample was evaporated to dryness and then taken up in toluene-d_8 and the ^{31}P spectrum recorded again

at 80 °C; the resonances of **4b** were δ 132.30 (s) and 75.10 (s), and those of **5a** were δ 179.04 (s) and 23.05 (s).

Partial Thermolysis of 3 in Solution. A 0.5 mL solution of **3** (0.030 g, 0.032 mmol) in toluene-d_8 was transferred into an NMR tube and heated at 80 °C for 5 min inside the NMR probe. A ^{31}P NMR spectrum (pulse delay 1 s) was then recorded. It showed the major resonances at δ 114.60 (s) and 80.00 (s) for compound **3** (66%) and resonances at δ 133.13 (s) and 75.73 (s) which were assigned to **4a** (34%). Heating at 80 °C was continued for an additional 5 min; the ^{31}P NMR spectrum then showed a decrease of **3** relative to **4a** and the presence of two further compounds (**4b** and **5a**). The new compounds showed resonances as follows: δ 132.30 (s) and 75.10 (s) (**4b**) and δ 179.04 (s) and 23.05 (s) (**5a**). The percentages of **3**, **4a**, **4b**, and **5a** were 26%, 67%, 4%, and 3%, respectively. After a further 5 min, small new resonances (for **5b**) appeared at δ 178.85 and 23.47; the relative percentages of the five compounds were 20%, 61%, 8%, 9%, and 2%, respectively. The sample was heated to 80 °C for another 10 min; the ^{31}P NMR spectrum then showed percentages of **3**, **4a**, **4b**, **5a**, and **5b** as 9%, 22%, 19%, 20%, and 30%, respectively. Finally, after a total of 50 min of heating, **3** had completely disappeared and **5b** had become the dominant product; the percentages were 5% (**4a**), 15% (**4b**), 17% (**5a**), and 63% (**5b**). Figure 3 gives a profile of these reactions. Note that, with all compounds, the upfield resonance (due to the ^{31}P resonance of the phosphine ligand) is broadened relative to that of the phosphite; however, the integrated areas are equal in each case.

Reaction of 4a with CO at Room Temperature. A concentrated solution of **4a** (0.030 g, 0.034 mmol in 0.5 mL of toluene) was transferred to an NMR tube. The solution was then saturated with CO by bubbling CO through it for 2 min. The tube was then capped, sealed with Parafilm, and allowed to stand at room temperature for 2 days. A ^{31}P NMR spectrum was then taken; it showed the relative percentages of **4a**, **3**, **4b**, and **5a** as 51%, 32%, 8%, and 9%, respectively.

Partial Thermolysis of 4a in Solution. A. With CO. A concentrated solution of **4a** (0.030 g, 0.034 mmol in 0.5 mL of toluene-d_8) was saturated with CO in an NMR tube. It was then heated to 70 °C in the NMR probe for 80 min. The ^{31}P NMR spectrum was recorded and showed the relative percentages of **4a**, **4b**, **5a**, and **5b** as 36%, 19%, 20%, and 25%, respectively.

B. Without CO. A concentrated solution of **4a** (0.030 g, 0.034 mmol in 0.5 mL of toluene) was transferred into an NMR tube and heated in the NMR probe for 80 min at 70 °C. After this time, the ^{31}P NMR spectrum showed that the relative percentages of **4a**, **4b**, **5a**, and **5b** were 72%, 11%, 13%, and 4%, respectively.

Attempted Thermolysis of 4a in the Solid State. A sample of **4a** (0.10 g, 0.11 mmol) was sealed in a glass tube, in vacuo, and heated to 85 °C for 3 days. The color changed slightly to a deep yellow, but NMR and IR spectra of this material were identical with those of compound **4a**.

Attempted Thermolysis of 5b in Solution. A. Without CO. A sample of **5b** (0.025 g, 0.028 mmol, in 0.5 mL of toluene-d_8) was placed in an NMR tube and heated to 50 °C for 40 min in the NMR probe. A ^{31}P NMR spectrum after this time showed **5b** together with a small amount of unidentified decomposition products. The sample was then heated to 70 °C for 30 min; again, the spectrum showed **5b** together with more decomposition products. After heating to 80 °C for 20 min, there was further decomposition but no isomerization products were evident.

B. With CO. A sample of **5b** (0.025 g, 0.028 mmol, in 0.5 mL of toluene-d_8) was placed in an NMR tube, the solution was saturated with CO, and then the sample was placed in the NMR probe and heated to 50 °C for 40 min. A ^{31}P NMR spectrum taken after this time showed only **5b** together with a small amount of unidentified decomposition products. The sample was then heated at 70 °C for 30 min; again only **5b** was present, but there was further decomposition. After 20 min at 80 °C, compound **5b** was still present, but more decomposition was evident. Another sample was prepared the same way but was heated at 40 °C for 16 h; the ^{31}P NMR spectrum taken after this time showed only **5b** together with some decomposition products.

Synthesis of *fac*-(η^5-C_5H_5)Fe(CO)(PPh_3)(CO_2)Re(CO)$_3$-[P(OEt)$_3$]$_2$ (6). In the glovebox, compound **4a** (0.40 g, 0.45 mmol) was dissolved in 10 mL of C_6H_6; P(OEt)$_3$ (0.08 g, 0.83 mL, 0.49 mmol) was added, and the mixture was stirred for 20 min. The solution changed from yellow to red; an IR spectrum showed that the starting material was gone. Solvent was evaporated from the reaction mixture, and the red residue was triturated with 60 mL of cold pentane at −60 °C, leaving a red-orange powder which was collected by filtration (0.42 g, 89% yield); mp 110−111 °C dec. Anal. Calcd for $C_{40}H_{50}FeO_{12}P_3Re$: C, 45.42; H, 4.76. Found: C, 45.63; H, 4.85. IR ν_{CO} (CH_2Cl_2): 2035 (s), 1964 (ms), 1900 (vs, br) cm^{-1}. IR ν_{OCO} (KCl, DRIFTS): 1510 (m), 1140 (m) cm^{-1}. ^{1}H NMR (CD_2Cl_2, −30 °C): δ 7.48 (br), 7.33 (br), 4.55 (m), 4.35 (s), 4.17 (m), 1.31 (t, J = 7.1 Hz), 1.26 (t, J = 7.1 Hz). ^{13}C NMR (CD_2Cl_2): δ 222.23 (d, J_{PC} = 34.2 Hz), 207.25 (dt, J_{PC} = 27.7 and 4.3 Hz), 192.84 (dd, J_{PC} = 96.3 and 13.3 Hz), 192.19 (dd, J_{PC} = 96.2 and 13.1 Hz), 191.83 (dd, J_{PC} = 10.5 and 10.5 Hz), 138.63 (d, J_{PC} = 40.8 Hz), 133.94 (d, J_{PC} = 9.8 Hz), 129.41 (d, J_{PC} = 1.7 Hz), 128.01 (d, J_{PC} = 9.3 Hz), 84.73 (s), 61.62 (t, J_{PC} = 4.4 Hz), 16.31 (d, J_{PC} = 4.0 Hz). ^{31}P NMR (toluene-d_8): δ 120.39 (d, J_{PP} = 50.9 Hz), 117.88 (d, J_{PP} = 50.8 Hz), 80.50 (s).

Attempted Thermolysis of 6 in the Solid State. A sample of **6** (0.20 g) was sealed, in vacuo, in a glass tube and heated to 60 °C for 4 h. After this time there was no change in the color and the IR spectral properties were unchanged. The sample was then heated to 85 °C; it changed to a dark residue after 6 h. The decomposition products could not be identified.

Reaction of 5b with HBF_4·EtO_2. In the glovebox, compound **5b** (0.16 g, 0.18 mmol) was dissolved in 10 mL of CH_2Cl_2 under nitrogen. HBF_4·EtO_2 (excess) was added, and the solution was stirred for 5 min. The mixture was then evaporated to dryness. Diethyl ether (20 mL) was added, and the soluble and insoluble portions were separated. The ether-insoluble portion was collected and dried under vacuum to leave an oily residue whose spectral properties were in agreement with those shown above for (η^5-C_5H_5)Fe(CO)$_2$[P(OEt)$_3$]$^+BF_4^-$. The ether-soluble product (Re product) was obtained as an oily residue after evaporating the solvent; it had the following spectral characteristics. IR ν_{CO} (CH_2Cl_2): 2038 (m), 1940 (s), 1910 (s) cm^{-1}. ^{1}H NMR (CD_2Cl_2): δ 7.46 (br). ^{13}C NMR (CD_2Cl_2): δ 191.84 (d, J_{PC} = 6.3 Hz), 188.36 (d, J_{PC} = 71.7 Hz), 133.46 (d, J_{PC} = 11.3 Hz), 131.23 (s), 129.27 (d, J_{PC} = 10.1 Hz), 128.87 (d, J_{PC} = 45.3 Hz). This product was not identified.

X-ray Crystal Structure of 4a. A suitable single crystal was grown by layering a 2:1 CH_2Cl_2/hexane solution (saturated) with hexane. Data were collected on an Enraf-Nonius CAD4 diffractometer as outlined in Table 1. Atomic positional parameters for the non-hydrogen atoms are given in Table 2. Selected bond distances and bond angles are shown in Table 3. Of 6473 unique reflections, 4273 were considered observed ($I > 3\sigma(I)$). The structure was solved using standard Patterson methods and refined with anisotropic thermal parameters for all non-hydrogen atoms while the calculated positions and thermal parameters for the hydrogen atoms were kept constant. The temperature factors of the hydrogen atoms were set to 1.2 times the temperature factors of the carbon atoms to which they were bonded. A final R index of 0.038 with R_w = 0.039 was obtained for 424 variables. All computations were performed using the teXsan[13] package (Molecular Structure Corp.).

Acknowledgment. Support of this work by the United States Department of Energy, Division of Chemi-

cal Sciences (Office of Basic Energy Sciences), Office of Energy Research, is gratefully acknowledged. The X-ray equipment was purchased with assistance from the National Science Foundation (Grant No. CHE-9016978). Support of the Molecular Structure Laboratory through the NSF/KY EPSCoR program (Grant No. EHR-9108764) is also gratefully acknowledged.

Supplementary Material Available: Tables of anisotropic thermal parameters, H atom positional parameters, bond distances, bond angles, and torsional angles for **4a** (11 pages). This material is contained in many libraries on microfiche, immediately follows this article in the microfilm version of the journal, and can be ordered from the ACS; ordering information is given on any current masthead page.

OM9405394